HOKKAIDO UNIVERSITY

Title	Influence of gas composition on the combustion and efficiency of a homogeneous charge compression ignition engine system fuelled with methanol reformed gases
Author(s)	Shudo, Toshio
Citation	International Journal of Engine Research, 9(5), 399-408 https://doi.org/10.1243/14680874JER01208
Issue Date	2008-10
Doc URL	https://hdl.handle.net/2115/35570
Type	journal article
File Information	JER9-5(MRG1-4).pdf

Hokkaido University Collection of Scholarly and Academic Papers : HUSCAP

Influence of gas composition on the combustion and efficiency of a homogeneous charge compression ignition engine system fuelled with methanol reformed gases

T Shudo
Division of Energy and Environmental Systems, Hokkaido University, N13 W8, Sapporo 060-8628, Japan,
email: shudo@eng.hokudai.ac.jp

The manuscript was accepted after revision for publication on 9 June 2008.

DOI: 10.1243/14680874JER01208

Abstract: A homogeneous charge compression ignition (HCCI) engine system fuelled with dimethyl ether (DME) and methanol-reformed gas (MRG), both produced from methanol by onboard reformers using exhaust heat, has been proposed in previous research. Adjusting the proportions of DME and MRG with different ignition properties effectively controlled the ignition timing and load in HCCI combustion. The use of the single liquid fuel, methanol, also eliminates the inconvenience of carrying two fuels while maintaining the effective ignition control effect. Because reactions producing DME and MRG from methanol are endothermic, a part of the exhaust gas heat energy can be recovered during the fuel reforming. Methanol can be reformed into various compositions of hydrogen, carbon monoxide, and carbon dioxide. The present paper aims to establish the optimum MRG composition for the system in terms of ignition control and overall efficiency. The results show that an increased hydrogen fraction in MRG retards the onset of high-temperature oxidation and permits operation with higher equivalence ratios. However, the MRG composition affects the engine efficiency only a little, and the MRG produced by the thermal decomposition having the best waste-heat recovery capacity brings the highest overall thermal efficiency in the HCCI engine system fuelled with DME and MRG.

Keywords: HCCI, methanol reformed gas, ignition control, hydrogen, DME, fuel reforming, waste heat recovery

1 INTRODUCTION

It is considered that the use of homogeneous charge compression ignition (HCCI) combustion in internal combustion engines will result in higher thermal efficiency and lower NO_x emissions as compared with conventional combustion systems. However, the difficulty of controlling the ignition timing in accordance with the engine load is preventing HCCI combustion from practical application to vehicles. Adjusting the proportion of two fuels with different ignition properties has been reported as a technique to control the ignition timing and load in HCCI combustion [**1**]. However, this technique has not been practically used in vehicles because of the inconvenience of carrying two kinds of fuel onboard.

Dimethyl ether (DME) has been studied as a clean alternative to diesel fuel owing to its high cetane number and smokeless combustion [**2**–**4**], and DME is produced simply from methanol by dehydration [**5**]. The idea of using a small amount of DME produced from methanol as an ignition-improving agent in a methanol direct-injection diesel engine has been reported [**2**]. Methanol can also be reformed into a mixture of hydrogen, carbon monoxide, and carbon dioxide. Since both hydrogen and carbon monoxide have good antiknock properties [**6**], methanol-reformed gases (MRGs) have been studied as fuels for spark-ignition (SI) engines [**7**–**8**].

With this background, an HCCI combustion engine system fuelled with DME and MRG has been proposed in a report [**9**]. The large reactivity

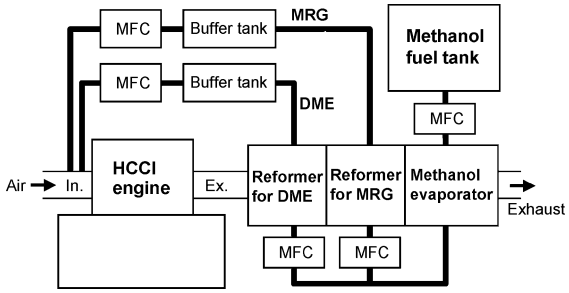

Fig. 1 Concept of the HCCI combustion engine system fuelled with DME and MRG onboard reformed from methanol

difference of the two fuels enables an effective control of the ignition timing by adjusting the proportions of the two in the system. In addition to the ignition control, the research has also proposed production of DME and MRG by onboard methanol-reformers utilising the exhaust heat from the engine as shown in Fig. 1. Catalytic reformers to produce DME and MRG are to be installed in the exhaust system just after the exhaust manifold for utilizing the high-temperature thermal energy of exhaust gas. Methanol evaporator in the downstream uses the exhaust gas heat at lower temperatures than the reformers. Because the reactions to produce DME and MRG from methanol are endothermic, the produced DME and MRG have higher heating values than liquid methanol. Theoretically, DME and MRG have higher LHV than methanol by 4 per cent and 20.1 per cent respectively. Therefore, the onboard methanol reformation can recover some of the waste heat from the engine. A combination of the high engine efficiency by HCCI operation and the waste heat recovery enables the HCCI combustion engine system to achieve higher overall thermal efficiency than conventional engine systems. The use of the single liquid fuel, methanol, also eliminates the inconvenience of carrying two fuels onboard and would make HCCI combustion of vehicles feasible. The higher energy density of liquid methanol compared to gaseous fuels is also advantageous to vehicle applications.

The previous research [**9**] used MRG by thermal decomposition that consists of 2 mol of hydrogen and 1 mol of carbon monoxide, and the hydrogen slows the autoignition of DME more effectively than carbon monoxide [**10**]. The hydrogen content of MRG can be varied by choosing reforming reactions. The current study aims to establish optimum compositions of MRG for the HCCI combustion engine system. The influences of the MRG composition on ignition, combustion, and thermal efficiency will be analysed in an HCCI combustion engine fuelled with DME and different types of MRG model gas. The possible overall thermal efficiency of the system is evaluated for different gas compositions under ideal reforming conditions.

Table 1 Specifications of tested engine

Engine type	Four-stroke cycle
Number of cylinder	Single
Bore × stroke	85 × 88 mm
Compression ratio	9.7:1
Supercharging	No
Intake heating	No
EGR	No

2 EXPERIMENTS

The experiments used a four-stroke cycle single-cylinder engine with a bore of 85 mm and a stroke of 88 mm as shown in Table 1. The engine has a flat top piston and a compression ratio of 9.7: 1. This relatively low compression ratio was shown to result in the optimal for thermal efficiency in a previous report [**9**] on DME-MRG HCCI combustion. Figure 2 shows the experimental system. Fuel gases were continuously supplied to the intake manifold of the engine from high-pressure cylinders. The flowrates of the fuels were controlled by needle valves and measured by Oval mass-flow meters (MFMs); the intake air was measured by an Oval MFM. The in-cylinder pressure was measured with an AVL piezo-electric type pressure-transducer installed in the cylinder head as shown in Fig. 3. For each experimental condition, 100 cycles of the pressure data were averaged and used to calculate the indicated mean effective pressure (i.m.e.p.), the indicated thermal efficiency, and the apparent rate of heat release. The concentrations of CO, THC, and O_2 in the exhaust gas were measured with NDIR, FID, and MPA-type analysers in a Horiba emission bench. For all the experiments, the engine speed was set at 1000 r/min, and the volumetric efficiency was set at 65 per cent including the fuel gases. The intake air

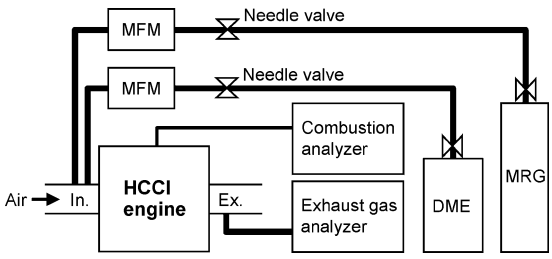

Fig. 2 Experimental system using model gases

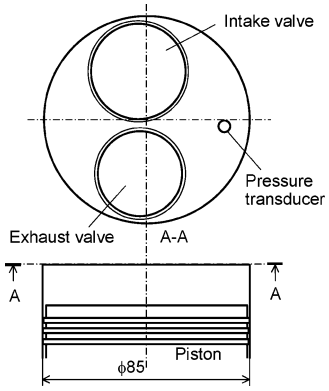

Fig. 3 Combustion chamber of the tested engine

was at room temperature and EGR was not applied to the engine.

3 REFORMING REACTIONS AND TESTED FUELS

Dimethylether (DME; CH_3OCH_3) is simply produced with high conversion ratios by the dehydration of methanol at temperatures above 450 K on a catalyst

$$CH_3OH \rightarrow 0.5CH_3OCH_3 + 0.5H_2O;\ \Delta H = 25.9\ \text{kJ} \quad (1)$$

Because the above dehydration reaction is endothermic, the produced $0.5CH_3OCH_3$ has a 4 per cent larger heating value than liquid CH_3OH. Methanol can also be thermally decomposed into hydrogen and carbon monoxide by the following catalytic reaction at temperatures above 500 K

$$CH_3OH \rightarrow 2H_2 + CO;\ \Delta H = 128.5\ \text{kJ} \quad (2)$$

This endothermic reaction turns 1 mol of methanol with the heating value of 638.1 kJ into reformed gas which has a total heating value of 766.6 kJ, 20.1 per cent higher than that of the liquid methanol. The carbon monoxide in the reformed gas can also be turned into hydrogen and carbon dioxide by the following water–gas shift reaction

$$CO + H_2O \rightarrow CO_2 + H_2;\ \Delta H = -41.2\ \text{kJ} \quad (3)$$

The overall reaction for producing the largest amount of hydrogen from methanol is as follows

$$CH_3OH + H_2O \rightarrow CO_2 + 3H_2;\ \Delta H = 87.3\ \text{kJ} \quad (4)$$

Because reaction (3) is exothermic, the increase in the heating value by reaction (4), steam reforming, is lower than reaction (2), thermal decomposition. By adjusting reactions (2) and (3), the proportion of H_2 and CO can be varied from 67:33 to 100:0, and the heating value can be increased from 20.1 per cent to 13.7 per cent through the reformation.

Table 2 Compositions and heating values of the tested methanol-reformed gases

	MRG1	MRG2	MRG3	MRG4
H_2	0.67	0.70	0.73	0.75
CO	0.33	0.18	0.08	0.00
CO_2	0.00	0.12	0.19	0.25
LHV (KJ/mol_{MeOH})	766.6	750.7	737.6	725.4

Instead of using the actual reformed gases, four types of model gas simulating MRG were used in the experiments. The compositions of the tested fuel gases are specified in Table 2. The paper denotes these as MRG1, MRG2, MRG3, and MRG4 respectively. The waste heat recovery effect was calculated based on ideal reforming conditions for each case.

4 RESULTS AND DISCUSSION

4.1 Characteristics of HCCI combustion of DME and MRG

Figure 4 shows the i.m.e.p., the indicated thermal efficiency η_i, and the exhaust emissions in HCCI combustion of DME and MRG1 with DME:MRG ratios of 100:0, 60:40, 50:50, and 40:60. A larger MRG fraction enables a richer mixture operation and increases i.m.e.p.. The HCCI combustion demonstrates the high thermal efficiency over a wide range of equivalence ratios. The exhaust emissions of THC and CO tend to decrease as the equivalence ratio increases. Figure 5 shows the in-cylinder pressure P and the apparent rate of heat release $dQ/d\theta$ for the four DME:MRG ratios in the results in Fig. 4 at the optimum equivalence ratios for thermal efficiency. Figure 5 clearly shows a two-stage heat release by the low-temperature oxidation reactions and the high-temperature oxidation reactions for each case. The second-stage heat release is strongly influenced by the DME:MRG ratio, while the timing of the first-stage heat release is weakly influenced by the DME:MRG ratio. An increased MRG retards the second-stage heat release, which is the main heat release, and this can effectively control the HCCI combustion phase. The retarded ignition timing allows operations at higher equivalence ratios without causing a too-high pressure rise. This is why the operational range of equivalence ratios was extended by adjusting the DME:MRG ratio in the HCCI combustion shown in Fig. 4.

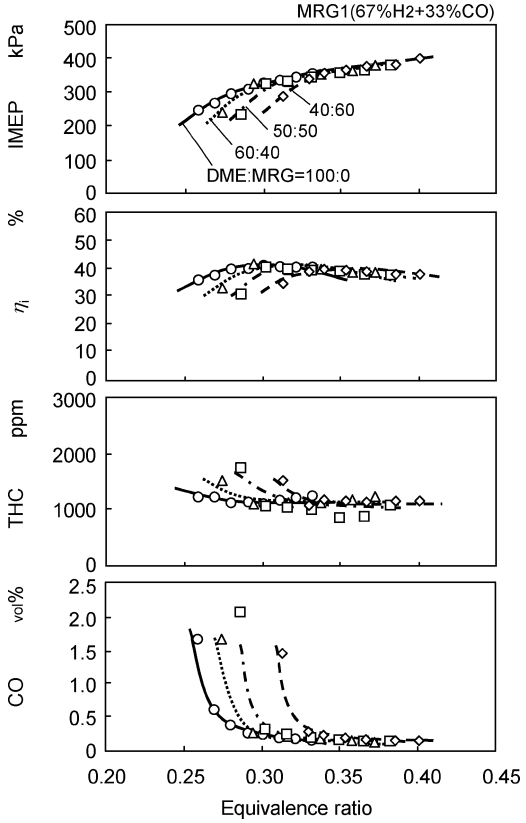

Fig. 4 i.m.e.p., indicated thermal efficiency, and exhaust emissions in HCCI combustion of DME and MRG1

4.2 Influence of hydrogen in MRG on autoignition of DME

Figure 6 shows the in-cylinder pressure and the apparent rate of heat release for HCCI combustion of DME and the four types of MRG at the equivalence ratio of $\phi = 0.38$ and the DME:MRG ratio 40:60. The

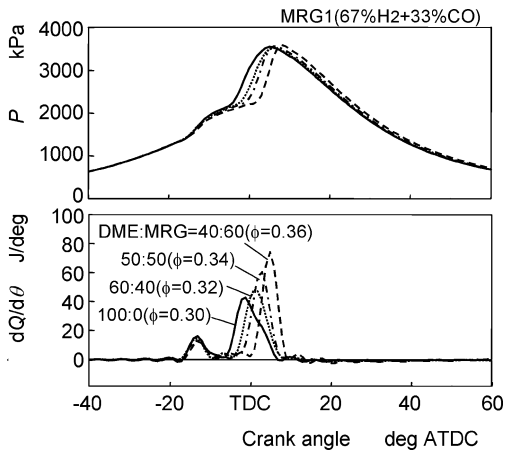

Fig. 5 Indicator diagrams for HCCI combustion of DME and MRG1 at optimum equivalence ratios for thermal efficiency

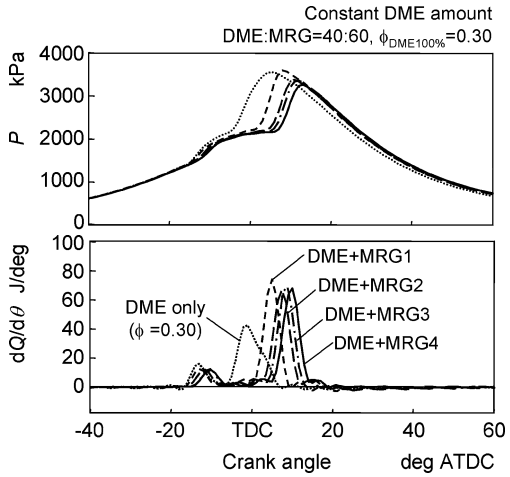

Fig. 6 Ignition control effects by addition of the MRG to HCCI combustion of DME at constant DME amounts

result without MRG at the equivalence ratio of $\phi = 0.30$, which has the same DME amount as the four cases with MRG, is also shown in the figure. All four cases with MRG retarded the combustion phase considerably as compared to the case without MRG, in spite of the increased equivalence ratios. The HCCI combustion of DME and MRG4, which contains the highest fractions of hydrogen and carbon dioxide, has the most retarded timing of the second-stage heat release. The effects of hydrogen and carbon monoxide, which are the flammable contents in the MRG, on HCCI combustion of DME are shown in Fig. 7. The equivalence ratio was at $\phi = 0.30$ for the case with DME only. The ratio of DME and hydrogen or carbon monoxide is 40:60, which brings the equivalence ratio to $\phi = 0.38$. The

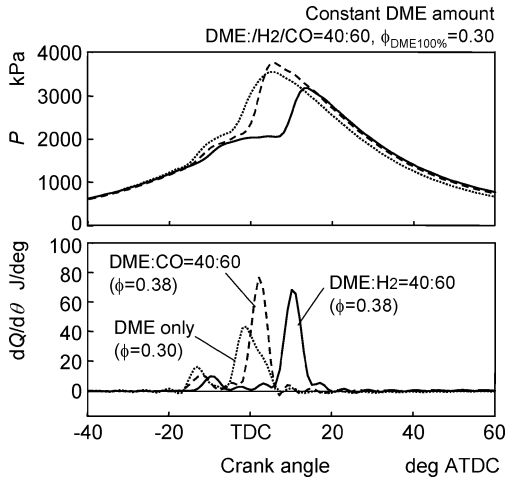

Fig. 7 Ignition control effects by additions of hydrogen and carbon monoxide to HCCI combustion of DME at constant DME amounts

figure clearly shows that hydrogen has a far stronger effect to retard the onset of the second-stage heat release by the high-temperature oxidation than carbon monoxide [**10**].

The detailed reaction mechanism for DME oxidation reported by Curran *et al.* [**11**–**12**] is often used to simulate the DME HCCI combustion processes. Calculations using this mechanism are able qualitatively to reproduce the trend of ignition timings in DME HCCI engine experiments with different equivalence ratios [**13**]. The first step of the mechanism is the H abstraction from DME producing CH_3OCH_2. In the low-temperature oxidation of DME, most of the CH_3OCH_2 is produced in the following H abstraction reaction by OH

$$CH_3OCH_3 + OH \rightarrow CH_3OCH_2 + H_2O \quad (5)$$

The CH_3OCH_2 reacts with O_2 or a third body to produce HCHO, OH, and other species. Then, the produced HCHO consumes OH

$$HCHO + OH \rightarrow CHO + H_2O \quad (6)$$

The OH is the chain carrier in the low-temperature oxidation. As a result of production and consumption of the OH, the chain branching terminates when $d[OH]/dt$ turns negative. When hydrogen is introduced to the low-temperature oxidation process of DME, H_2 consumes OH as in equation (7) [**13**]

$$H_2 + OH \rightarrow H_2O + H \quad (7)$$

$$CO + OH \rightarrow CO_2 + H \quad (8)$$

Reaction (7) proceeds at a three to six times higher rate than reaction (8) in the temperature range from 700 to 1000 K, where the low-temperature oxidation reactions occur, as shown in Fig. 8. This causes the differences in the ignition control effect of hydrogen

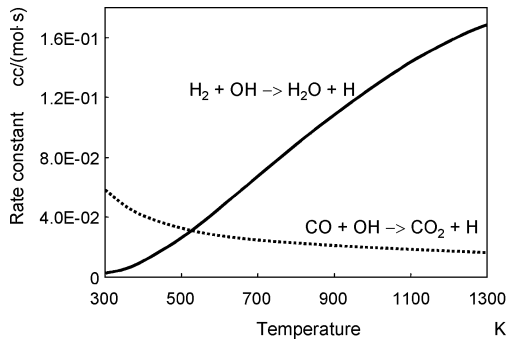

Fig. 8 Rate constants for $H_2 + OH$ and $CO + OH$

and carbon monoxide. The H produced from reactions (7) and (8) quickly recombines with O_2 producing HO_2, then HO_2 reacts with H to produce H_2O_2. The HO_2 and H_2O_2 are much less reactive than OH during the low-temperature oxidation process

$$H + O_2 + M \rightarrow HO_2 + M \quad (9)$$

$$HO_2 + H \rightarrow H_2O_2 \quad (10)$$

The significant retardation in low-temperature oxidation by the addition of hydrogen shown in Fig. 7 is attributed to the consumption of OH by H_2 [**13**]. The OH consumption reduces the OH concentration and $d[OH]/dt$ and retards the H abstraction from CH_3OCH_3 by OH, which is the dominant reaction in the early step of the low-temperature oxidation of DME. Subsequently, this delays the heat release and the temperature rise during the low temperature reactions.

Figure 9 shows the influence of hydrogen addition on the mol fractions of chemical species and temperature against crank angle in DME HCCI combustion. The calculations employed the DME oxidation mechanism by Curran *et al.* [**12**] Volume changes and initial conditions for the calculation were determined from the engine experiments. Calculation conditions for H_2/DME mol fraction are 0, 1.0, and 1.5 with a constant DME amount which brings an equivalence ratio of $\phi = 0.27$ in the neat DME case. The increase in hydrogen decreases the OH concentration remarkably and retards the first peak of the OH concentration, and this subsequently retards consumption of CH_3OCH_3 and formation of HCHO. The high-temperature oxidation starts with the dissociation of H_2O_2 to 2OH and oxidizes intermittent species to H_2O and CO_2. The H_2O_2 decreases and OH increases rapidly at around 1100 K, regardless of the hydrogen fraction; along with the abrupt increase in the OH concentration, CH_3OCH_3 is rapidly consumed.

Figure 10 shows the crank angles at the beginning of the first-stage heat release by the low-temperature oxidation reactions, θ_{LTR}, and at the second-stage heat release by the high-temperature oxidation reactions, θ_{HTR}, for the experimental results in Figs 6 and 7. The values are shown against the hydrogen fraction in the MRG. The MRG composition versus the hydrogen fraction is also shown in the figure. The figure shows that the onsets of both the first and second heat releases retard with increases in the hydrogen fraction. The MRG4 with the highest hydrogen fraction results in the strongest ignition retardation effect.

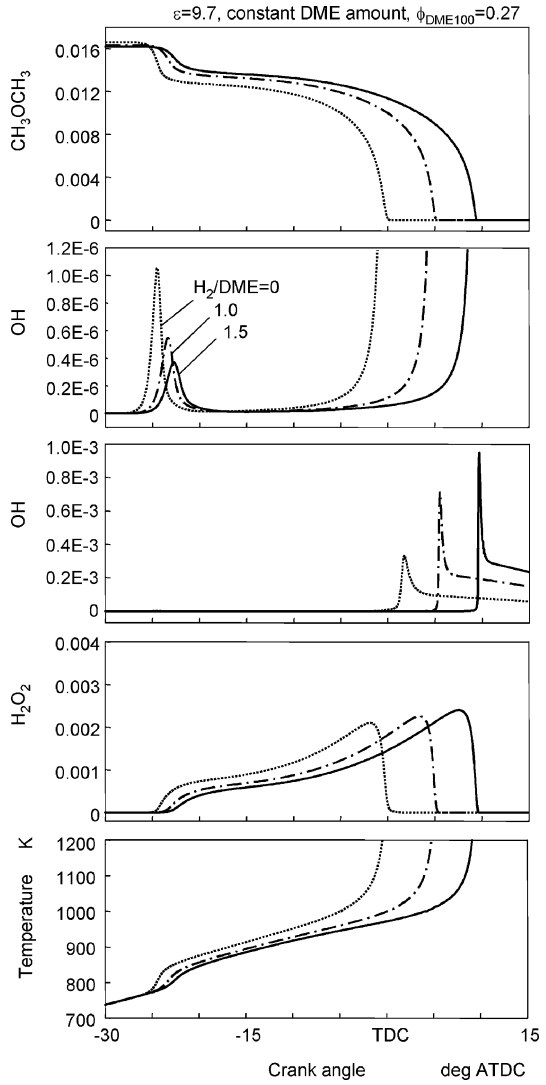

Fig. 9 Calculated mole fraction of species and temperature in DME HCCI combustion with different hydrogen fractions

4.3 Influence of CO_2 on autoignition of DME

With increases in the hydrogen fraction, carbon monoxide decreases and carbon dioxide increases in the MRG. Carbon dioxide is almost an inert gas at the low-temperature oxidation conditions and it has little direct influence on the oxidation reaction process of DME but its large heat capacity may influence the ignition process. Figure 11 shows the influence of carbon dioxide on the HCCI combustion of DME at an equivalence ratio of $\phi = 0.28$. The influence of nitrogen at the same condition is also shown in the figure for comparison. In the condition of the constant equivalence ratio and DME amount, the addition of carbon dioxide retards the ignition timing because of the delayed temperature rise by the increased heat capacity of the mixture slightly.

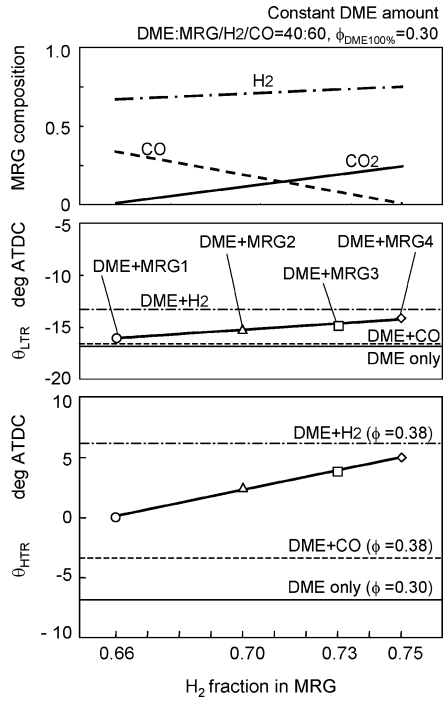

Fig. 10 Influence of MRG composition on the onsets of the low and high-temperature oxidation reactions in HCCI combustion of DME

While the ignition control effect is smaller than that of hydrogen or carbon monoxide, the effect by the MRG shown in Fig. 10 is also attributed to the higher heat capacity of carbon dioxide. This also suggests the ignition control effect by external EGR.

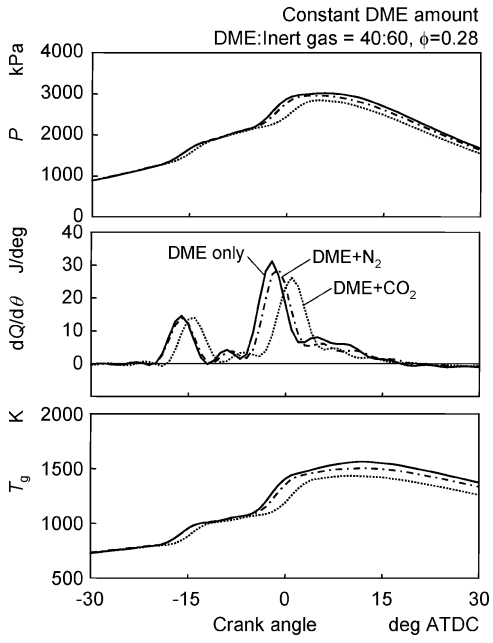

Fig. 11 Influence of heat capacity of mixture on HCCI combustion of DME

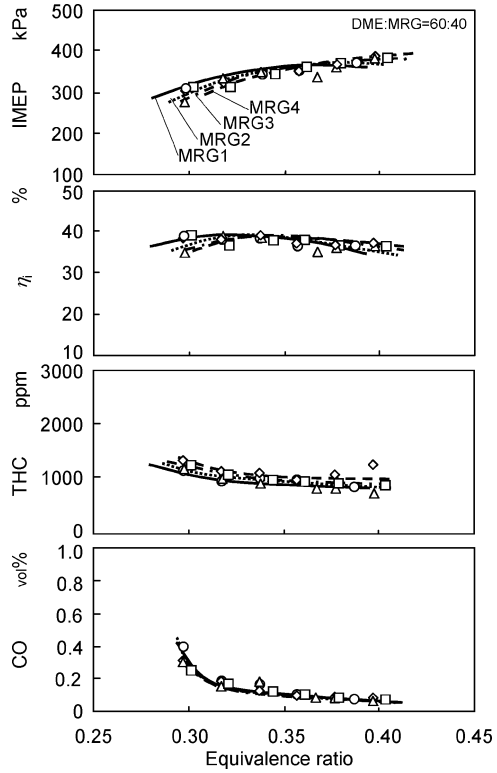

Fig. 12 HCCI combustion of DME and the four types of MRG

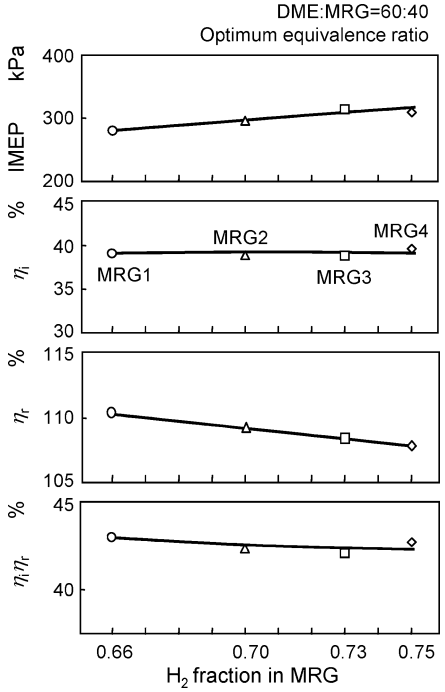

Fig. 13 Influence of MRG composition on the overall thermal efficiency including heat recovery through methanol reforming

4.4 Comparison of HCCI combustion of DME and the four types of MRG

Figure 12 shows the i.m.e.p. and the exhaust emissions in HCCI combustion of DME and the four types of MRG. The DME:MRG ratio was set at 60:40, the optimal for thermal efficiency. An MRG with a higher hydrogen fraction tends to have the peak thermal efficiency at higher equivalence ratios. This is attributed to the more retarded combustion phase by the higher hydrogen fraction. Because of this, the case with the higher hydrogen fraction has slightly higher i.m.e.p. at higher equivalence ratios. THC and CO exhaust emissions tend to decrease as the equivalence ratio increases. This can be attributed to temperature increases due to the increased equivalence ratio. THC exhaust emissions tend to increase slightly with the hydrogen fraction in the MRG. There is almost no influence of MRG-type on CO emissions, suggesting that a large part of the unburned CO originates from the DME.

4.5 Overall thermal efficiency based on methanol

As described in section 2, DME and MRG, which are produced from methanol, have higher heating values than the liquid methanol. The utilization of the engine exhaust gas heat for the endothermic reforming reactions could be applied to recover part of the waste heat from the engine. This research introduces an index η_r to express the degree of increase in the heating value by the fuel reforming. Multiplying the degree of heat increase η_r by the engine efficiency η_i gives the overall thermal efficiency of the system including the waste heat recovery effect by the fuel reforming using the engine exhaust gas heat

$$\eta_{overall} = \eta_r \eta_i \tag{11}$$

This factor is the energy conversion efficiency from the LHV of supplied liquid methanol fuel to the engine work.

Figure 13 shows the overall thermal efficiency $\eta_r\eta_i$ for some of the experimental data in Fig. 12. The degree of heat increase during the fuel reforming η_r was calculated for ideal reforming reactions. It was assumed that the heat required for the reactions was provided by the engine exhaust gas. The values of the engine efficiency η_i shown in the figure are at the equivalence ratios that are optimum for the thermal efficiency for each MRG type. The highest degree of heat increase is achieved with MRG1, that is produced by the thermal decomposition in reaction (2). Because of the small differences in engine efficiency among the four cases, the overall thermal

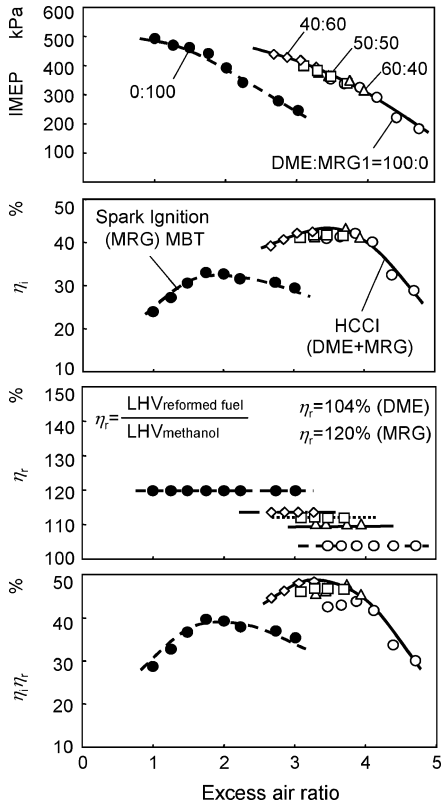

Fig. 14 Overall thermal efficiency

efficiency $\eta_r\eta_i$ is the highest with MRG1. Although MRG4 with the highest hydrogen fraction by reaction (4) has the strongest effect to control ignition and can produce the highest i.m.e.p., MRG4 results in lower overall thermal efficiency than MRG1 owing to the lower η_r.

Figure 14 shows the overall thermal efficiency versus excess air ratio for HCCI combustion of DME and MRG1 under various operating conditions. For comparison, results of the homogeneous charge SI combustion are also shown in the figure. Because of the necessity for high antiknock properties, the SI combustion was fuelled with MRG1 only. Ignition was provided by a spark discharge in the central position of the combustion chamber, and set at optimum timings for the indicated thermal efficiency. The thermal efficiency of the HCCI combustion is significantly higher than that of the SI combustion in leaner mixture conditions. Because of the higher thermal efficiency, the i.m.e.p. of HCCI combustion is comparable to that of SI combustion in spite of the lean operation. Because the degree of heat increase η_r is higher for the MRG1 production compared with the DME production, conditions with a larger amount of MRG1 have advantages in terms of the exhaust heat recovery. The SI combustion, which is fuelled with neat MRG1, has a higher waste heat recovery effect than the HCCI combustion of DME and MRG1. However, the overall efficiency $\eta_r\eta_i$ of the HCCI combustion is higher than that of SI combustion, because of the higher engine efficiency by the HCCI operation and the effective exhaust heat recovery. This study set the rich side operation limits of the HCCI operation with the maximum rate of pressure rise of 300 kPa/degrees CA. While the maximum operable equivalence ratio was around 0.4 owing to this criterion, higher engine-load operation will be achievable with HCCI combustion if a maximum rate of pressure rise higher than this value is permitted.

To confirm the effectiveness of the exhaust gas heat recovery, energy balances in the onboard fuel reforming system accommodated in the HCCI engine system are calculated. Figure 15 shows a typical example of the results obtained at a condition of 43 per cent indicated thermal efficiency and a DME:MRG ratio of 40:60. When methanol with a heating value of 100 J is used, total heating value of reformed gases is increased to 113.2 J by way of evaporation and reformation utilizing the exhaust gas heat. The HCCI engine fuelled with 113.2 J input produces 49 J indicated output work and 36 J exhaust gas heat. The two reformers use 21.1 per cent of the exhaust heat, and the evaporator, which is placed downstream of the reformers, uses 19.7 per cent of the rest of the exhaust heat.

It is confirmed from the above discussion that the newly proposed HCCI combustion engine system that recovers the exhaust heat using two onboard fuel reformers is an efficient and clean energy system. The use of a single liquid fuel, methanol, also eliminates the inconvenience of carrying two fuels while maintaining flexible ignition control by varying the combination of the two reformed fuels with different ignition properties. The higher energy density of liquid methanol is also an advantage over gaseous fuels.

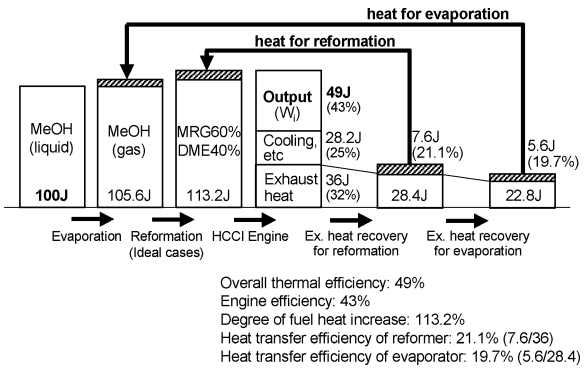

Fig. 15 Typical example of heat balances

5 CONCLUSIONS

The results obtained in this research may be summarized as follows.

1. The HCCI combustion engine system which recovers the waste heat by onboard fuel reforming is an efficient and clean system. The use of the single liquid fuel, methanol, also eliminates the inconvenience of carrying two fuels while maintaining the effective ignition control effect by the combination of two reformed fuels with different ignition properties.
2. In HCCI combustion of DME and MRG, an increased hydrogen fraction in MRG retards the timing of the second-stage heat release by high-temperature oxidation reactions and permits operation with higher equivalence ratios.
3. The addition of carbon dioxide retards the auto-ignition of DME slightly because of a delayed temperature rise due to its large heat capacity. The ignition control effect by the MRG with higher hydrogen fractions is also attributed to carbon dioxide that increases with the hydrogen fraction.
4. The optimum equivalence ratio for thermal efficiency tends to increase as the fractions of hydrogen and carbon dioxide in the MRG increase; however, the MRG composition affects the peak engine efficiency only a little.
5. Because of the small influence of MRG composition on engine efficiency, the MRG produced by the thermal decomposition reaction having the best waste-heat recovery capacity results in the highest overall thermal efficiency in the HCCI combustion engine system fuelled with DME and MRG.

ACKNOWLEDGEMENTS

The author thanks Mr Takehiro Takahashi, Mr Shinichi Iio, and Mr Tomoyuki Yokoyama, former students of Musashi Institute of Technology, for their help in the experiments. This research was supported by the RC193 and RC210 of the Japan Society of Mechanical Engineers. The author expresses gratitude to Professor Kamimoto, the editor of *International Journal of Engine Research*, for reading the manuscript and making helpful suggestions.

REFERENCES

1 **Furutani, M., Ohta, Y., Kono, M.,** and **Hasegawa, M.** A Ultra-lean premixed compression-ignition engine concept and its characteristics. In Proceedings of COMODIA 98, 1998.

2 **Murayama, T., Chikahisa, T., Guo, J.,** and **Miyano, M.** A study of compression ignition methanol engine with converted dimethyl ether as an ignition improver. SAE paper 922212, 1992.

3 **Sorenson, S. C.** and **Mikkelsen, S. E.** Performance and emissions of a 0.273 liter direct injection diesel engine fuelled with neat dimethyl ether. SAE paper 950064, 1995.

4 **Kajitani, S., Chen, Z., Konno, M.,** and **Rhee, K. T.** Engine performance and exhaust characteristics of direct-injection diesel engine operated with DME. SAE paper 972973, 1997.

5 **Bercic, G.** and **Levec, J.** Catalytic dehydration of methanol to dimethyl ether kinetic investigation and reactor simulation. *Ind. Engng Chem. Res.*, 1993, **32**

6 **Obert, E. F.** *Internal combustion engines and air pollution*, 1973 (Harper & Row, New York).

7 **Hirota, T.** Study of methanol-reformed gas engine. *J. SAE Japan*, 1980, **34**(10).

8 **Shudo, T., Tsuga, K.,** and **Nakajima, Y.** Combustion characteristics of H_2-CO-CO_2 mixture in an IC engine. *SAE Trans. J. Engines*, 2002, **110**(3).

9 **Shudo, T.** and **Ono, Y.** HCCI combustion of hydrogen, carbon monoxide and dimethyl ether. *SAE Trans. J. Engines*, 2003, **111**(3).

10 **Shudo, T., Ono, Y.,** and **Takahashi, T.** Influence of hydrogen and carbon monoxide on HCCI combustion of dimethyl ether. *SAE Trans. J. Fuels Lubricants*, 2003, **111**(4).

11 **Fischer, S. L., Dryer, F. L.,** and **Curran, H. J.** Reaction kinetics of dimethyl ether. I: High-temperature pyrolysis and oxidation in flow reactors. *Int. J. Chem. Kinetics*, 2000, **32**.

12 **Curran, H. J., Fischer, S. L.,** and **Dryer, F. L.** The reaction kinetics of dimethyl ether. II: Low-temperature oxidation in flow reactors. *Int. J. Chem. Kinetics*, 2000, **32**.

13 **Shudo, T.** and **Yamada, H.** Hydrogen as an ignition-controlling agent for HCCI combustion engine by suppressing the low-temperature oxidation. *Int. J. Hydrogen Energy*, 2007, **32**.

BIBLIOGRAPHY

Shudo, T., Nabetani, S., and **Nakajima, Y.** Analysis of the degree of constant volume and cooling loss in a spark ignition engine fuelled with hydrogen. *Int. J. Eng. Res.*, 2001, **2**(1).

Shudo, T., Ono, Y., and **Takahashi, T.** Ignition control by DME-reformed gas in HCCI combustion of DME. *SAE Trans. J. Fuels Lubricants*, 2004, **112**(4).

APPENDIX

Notation

ATDC	after top dead centre

$dQ/d\theta$	apparent rate of heat release	Q	cumulative apparent heat release
DME	dimethylether	SI	spark ignition
EGR	exhaust gas recirculation	T_g	in-cylinder gas mean temperature
HCCI	homogeneous charge compression ignition	THC	total hydrocarbon
HTR	high-temperature oxidation reactions	ΔH	enthalpy
i.m.e.p.	indicated mean effective pressure	η_i	indicated thermal efficiency
LHV	lower heating value	η_r	degree of heat increase by fuel reforming
LTR	low-temperature oxidation reactions		
MeOH	methanol	$\eta_i\eta_r$	overall thermal efficiency
MFC	mass flow controller	θ	crank angle
MFM	mass flow meter	θ_{HTR}	crank angle at start of HTR
MRG	methanol-reformed gas	θ_{LTR}	crank angle at start of LTR
P	in-cylinder pressure	ϕ	equivalence ratio